

Aquaporin 4 expression after ischemic stroke

A literature review on the temporal and spatial regulation of Aquaporin 4 expression after Ischemic stroke and its consequences for stroke pathophysiology

Shervin Banitalebi

Medicine

20 Credits

Institute of Basic Medical Sciences

Faculty of Medicine



Abstract

Ischemic stroke, accounting for 87% of stroke cases globally is a considerable source of morbidity and mortality. After the initial thromboembolism of a cerebral vessel, secondary injuries such as oedema and reactive gliosis occur as a part of the pathophysiology of stroke. Aquaporin-4 (AQP4) is the primary water channel found in the brain and is highly expressed on astrocyte endfeet surrounding blood vessels in the brain. Disruption of this perivascular expression of AQP4 is seen across multiple chronic and acute neurologic illnesses, including ischemic stroke. As AQP4 is a water channel it has been studied as an important factor in stroke pathology, especially in the context of oedema. More recently, it is becoming apparent that AQP4 also has a role in reactive gliosis. Therefore, a literature review was conducted to compile our current knowledge on the expression and disruption of AQP4 after both experimental stroke in mice, and in clinical and pathohistological research on humans. Data from experimental stroke in mice show changes in AQP4 expression as well as perivascular polarization in the first hours to days after infarction. These changes follow logically as responses to oedema formation. While studies on human samples show a loss of perivascular AQP4 and an increase in the total amounts of Aquaporin 4 in the glial scar in the chronic stages after stroke, which could have structural implications for the glial scar. Overall, AQP4 expression changes on the temporal and spatial dimensions in relation to the secondary injuries seen after stroke.

Index

Abstract.....	1
1 – Introduction.....	3
1.2 – Clinical aspects of stroke	3
1.3 – Aquaporin-4 and Astrocytes	5
1.4 – The involvement of Aquaporin-4 in ischemic stroke.....	7
1.4 – The Blood-Brain Barrier and brain oedema	7
1.5 – Innate neuroinflammation and astrogliosis	10
1.6 – Sexual dimorphisms of the brain	11
1.7 – Experimental stroke and comparative medicine	11
2 – Methods	12
2.1 – Search method and criteria.....	12
2.2 – Comparing quantitative data	14
2.3 – Strain, age and sex in animal experiments	15
3 – Results.....	17
3.1 – AQP4 in Human stroke	17
3.2 – AQP4 Protein expression in experimental stroke	18
3.3 – AQP4 mRNA expression in experimental stroke	26
4 – Discussion.....	27
4.1 – AQP4 in stroke research	27
4.2 – The relation of AQP4 expression to Oedema and astrogliosis	28
4.3 – Plausible mechanisms of AQP4 disruption.....	29
4.4 – Short comings of experimental stroke research	30
5 – Conclusion	30
References.....	31

Abbreviations: Aquaporin 4 (AQP4), Central Nervous System (CNS), Dystrophin Associated Protein Complex (DAPC), alpha-syntrophin (a-syn), National Institute of Health Stroke Score (NIHSS), modified Rankin scale (mRS), Barthel index (BI), cerebrospinal fluid (CSF), Blood-Brain Barrier (BBB), Middle cerebral artery (MCA), Proximal middle cerebral artery occlusions (pMCAO), distal middle cerebral artery occlusion (dMCAO), quantitative polymerase chain reaction (qPCR), sodium dodecyl sulfate–polyacrylamide gel electrophoresis (SDS-PAGE), Blue Native–polyacrylamide gel electrophoresis (BN-PAGE), Glial Fibrillary Acidic Protein (GFAP)

1 – Introduction

Ischemic stroke, caused by arterial embolism, is the most common subtype of stroke representing 87% of stroke cases globally (1,2). Following is haemorrhagic stroke, caused by a bleeding cerebral artery, which accounts for 13% of stroke cases (1). There are also rarer aetiologies such as cerebral venous embolism leading to venous stasis ischemia. Regardless of aetiology, stroke alone represents a considerable health burden, and is a major contributor to morbidity as well as mortality, especially in the developing world (2).

For this review, we will only consider ischemic stroke as it is the most common type of stroke. While the mode of primary injury differs between the different types of stroke, they share some of the same secondary injuries. Particularly oedema and acute inflammation are present shortly after the onset of both ischemic and haemorrhagic stroke (3,4). The extent and composition of secondary injuries may vary between types of stroke and are dependent factors such as the extent of the primary insult. Nevertheless, secondary injuries give rise to significant sequela of the individual stroke patient.

1.2 – Clinical aspects of stroke

The brain as an organ is highly sensitive to hypoperfusion. This is best exemplified by prioritization of cardiac output to brain perfusion (5). The loss of perfusion, as seen in ischemic stroke, results in neuronal dysfunction and ultimately cell death. An infarct core is quickly established as a focal lesion after an embolism, setting the baseline damage that cannot be avoided. In the acute phase, the penumbra surrounds the infarction core. The penumbra is a zone of partial hypo-perfusion, characterized by metabolic dysfunction (6). This zone is temporary in nature and may resolve in one of two ways. First, with sufficient time under hypo-perfusion the tissue will become necrotic, and thus enlarging the infarction core. Second, tissue may be spared, either through timely reperfusion treatment, or by the brain's own collateral arterial supply (6). Hence, the degree of irreversible tissue damage is mainly dependent on two factors: time, and the anatomical localization of the embolus.

In clinical practice, as well as in clinical research, multiple scoring tools have been developed to identify stroke and follow its progression in patients. Among these, the National Institute of Health Stroke Score (NIHSS) is one of the more common in use today. The main advantages of NIHSS is its value in early detection of stroke, as well as its use in serial

assessment during the hospital stay (7). NIHSS is also preferred in stroke research to the other scores such as modified Rankin scale (mRS), and Barthel index (BI) due to its higher sensitivity. These scoring systems are one of the core measurements in therapeutic as well as prognostic studies.

Treatment of the primary injuries in ischemic stroke is highly time sensitive. Estimates show a loss of 2 million neurons each minute (8), making stroke treatment a race against time. Current guidelines give intravenous thrombolysis a window of 4.5 hours before the risk of cerebral haemorrhage becomes too great (9). The short window to act poses a great challenge, especially for rural and less developed communities. Globally only 5% of cases of ischemic stroke is treated with intravenous thrombolysis (2). Mechanical thrombectomy may be performed up to 24 hours after onset of ischemia. This method is restricted by multiple factors such as availability of the embolism for extraction (10). 10-20% of ischemic stroke is caused by large vessel occlusion (2), and these are the primary candidates for mechanical thrombectomy. However, the availability of mechanical thrombectomy is scarce and unevenly distributed. Of the around 2000 thrombectomy facilities in the world, 900 are in the United States of America (2).

Intravenous thrombolysis and mechanical thrombectomy are the only modes of re-establishing the local perfusion, and are highly effective when performed within the given time-limit. Paradoxically, reperfusion therapy may cause additional damage. Reperfusion injury occurs after successful intravenous thrombolysis or mechanical thrombectomy, and is mediated by the release of reactive oxygen species (ROS) from mitochondria leading to cell death (11). ROS damage to the BBB may cause a haemorrhagic transformation of the ischemic stroke, as well as lead to oedema (11).

Following the primary ischemic injuries to the brain is a range of secondary injuries or complications in the acute to sub-acute phase, as well as chronic sequela. Brain oedema is estimated to affect 22% of ischemic stroke patients (12), and is correlated with worse NIHSS scores (12,13). Another phenomenon is a loss of neurons after the initial ischemia adding to the irreversible damage. While the secondary neuronal loss may be caused by multiple factors, the innate inflammatory mechanisms of the brain are gaining more attention as a plausible mechanism. Treatment for oedema and inflammatory reactions remain elusive. Currently, decompressive craniectomy is the main treatment for brain herniation which may result from excessive oedema (14). The use of corticosteroids to prevent brain inflammation

and oedema remains controversial, and is therefore not standard practice (15). The lack of treatment for secondary injuries highlights the need to understand the basic pathophysiology of stroke.

1.3 – Aquaporin-4 and Astrocytes

Regulation of water transport across cellular membranes is a physiological need across prokaryotes and eukaryotes. Testament to this fact is the conservation of water channel expressing genes across the tree of evolution (16). Aquaporins are a family of transmembrane water channel proteins in mammalian cells first discovered by Peter Agre and co-workers (17). The first experiments confirming the existence and function of Aquaporin 1 showed its necessity in erythrocyte volume regulation in response to extracellular changes in osmolarity (18). Since then, 13 aquaporins (AQP0-AQP12) have been found in humans. These are divided into classical aquaporins (selective for water), Aquaglyceroporins (allowing glycerol and similar molecules), as well as superaquaporins (19,20). Aquaporin-4 (AQP4) at the molecular level is a classical aquaporin with a sufficiently small channel pore to allow a single file of water molecules to pass through (21). This allows for highly selective and rapid diffusion of water across the plasma membrane (20). AQP4 is highly expressed in the Central nervous system (CNS), primarily in astrocytes. However, it is also expressed in ependymal cells lining the ventricles and muller cells in retina (20).

In the plasma membrane AQP4 monomers assemble to form tetramers, and tetramers further assemble to form orthogonal arrays of particles (OAPs) (22). The size of OAPs is directly linked to the ratio of the main AQP4 isoforms, M23-AQP4 and M1-AQP4 (23). These isoforms are found in both mice and humans (22). The difference between the isoforms lies in the N-terminal with M23-AQP4 being 22 amino-acids shorter due to transcription starting on the second methionine codon in position 23 (24). In the brain the ratio of M23-AQP4 to M1-AQP4 is approximately 3:1 during normal physiological conditions (23). OAP formation is necessary for normal AQP4 expression in the brain (25) and may act as adhesion molecules stabilizing astrocytic processes (26). The formation of OAPs is also seen by AQP0 in the lens of the eye where it is essential for cell to cell adhesion (27). Taken together, OAPs are seemingly involved in cell to cell adhesion as long as the cells express the same OAP forming aquaporin. Looking at this from another perspective we see that the disruption or lack of AQP4 based OAPs promotes cell migration, as seen in reactive astrogliosis (28,29).

Astrocytes are one of the main components of the glial cells of the brain. Some of the main functions of astrocytes are: maintenance of extracellular water and ion homeostasis, metabolic support to neurons, clearance of neurotransmitters from synapses and reaction to damage in the process of reactive astrogliosis (30,31). To allow for these functions, astrocytes have a star-like morphology with multiple processes (30–32). Of special interest are the perivascular endfeet maintaining a complete cover of the brain vasculature (33), the sub-pial endfeet covering the brains surface, and the peri-synaptic processes taking part in the tripart synaptic model (34). Each domain has a polarized expression of proteins to enable the astrocytes functions.

Taking a closer look at the perivascular endfeet, we see a highly selective expression of AQP4 (20), as well as the other membrane proteins such as the potassium channel Kir4.1, in the adluminal endfoot membrane (35). This selective enrichment of these proteins is termed perivascular astrocyte polarization. And, as stated previously, the loss of astrocyte polarity is an hallmark of CNS pathology (36). Therefore, it is worth discussing the molecular basis of perivascular polarization. The Dystrophin associated protein complex (DAPC) is an intracellular complex of anchoring proteins based around the dystrophins DP71 and Dystrobrevin (37). This dystrophin backbone is connected to the cytoskeleton via actin, and the plasma membrane through dystroglycans (38). The DAPC is connected, through the extracellular part of dystroglycans, to laminin and agrin of the vascular basal lamina ensuring the perivascular polarization of the DAPC (38). Finally, alpha-syntrophin (a-syn) connects AQP4 to the DAPC, and therefore anchors AQP4 to the adluminal endfoot membrane (39). However, a direct connection between a-syn and AQP4 is yet to be established. Recently a new isoform of AQP4 was discovered. AQP4ex I takes its name due to an extended intracellular C-terminus (40), and is shown to be necessary for perivascular AQP4 polarization in the brain (41). Thus AQP4ex may serve as the missing link between the perivascular pool of AQP4 and a-syn. To summarize, genetic knock out experiments in mice show that DP71, a-syn, AQP4ex, laminin and agrin are all necessary for correct perivascular polarization of AQP4 (38,42,43).

Astrocytes are a heterogeneous cell population. Morphologically, astrocytes are divided into protoplasmic astrocytes residing in gray matter, and fibrous astrocytes residing in the white matter (30,31). Other members of the extended astroglia family are the muller cells of the retina, and Bergmanns glia in the cerebellum (44,45). There are also species-specific differences. In primates, but not rodents, interlaminar astrocytes reside in the cortex with

processes spanning across the layers of the cortex (30). With advances in single cell analysis it is becoming more evident that astrocytic heterogeneity goes further than their morphology, and specific subpopulations may differ in function (46). However, all astrocytes maintain a base level of homeostatic functions, and share the same gross anatomical organization (31). Processes from different astrocytes have little overlap, thus giving each astrocyte its own area of responsibility (31). Yet, astrocytes are connected to each other through connexin-43 and connexin-30 based gap-junctions allowing for communication over a larger astrocyte networks (47). Other connexins also allow for gap junctions connecting the astrocytes to oligodendrocytes (48) and astrocytes may release transmitters such as glutamate or ATP in signalling to neurons (34), further adding to the complexity of connections in the brain.

1.4 – The involvement of Aquaporin-4 in ischemic stroke

The role of AQP4 in stroke pathology is hotly debated, especially concerning its role in post-stroke oedema and neuroinflammation. Studies on experimental stroke show AQP4 to be important for both formation and resolution of oedema (49). And recent studies show the involvement of AQP4 in reactive astrogliosis which is an innate inflammatory process of the brain (50–53). A near universal hallmark of neuropathology (seen across both acute and chronic diseases such as; stroke, traumatic brain injury, mesial temporal lobe epilepsy, glioma and Alzheimer's disease) is the loss of perivascular AQP4 polarization in astrocyte endfeet (36). Taken together, these facts make AQP4 an attractive target for pharmacological intervention. Multiple AQP4 channel-blocking agents (54,55) and drugs targeting the subcellular localization (52) are being researched with promising preclinical results. However, plaguing stroke therapy research is a long line of drugs showing promise in preclinical trials and failing to deliver in clinical trials (56). For any AQP4 based intervention to succeed in clinical medicine, one must consider how stroke pathology effects the expression and distribution of AQP4. Therefore, we will shed light on the expression of AQP4 in both spatial and temporal dimensions, and how these relate to post stroke oedema and reactive astrogliosis.

1.4 – The Blood-Brain Barrier and brain oedema

First, it is important to consider the anatomy and physiology of fluid movement in the brain. The fluid compartments of the brain are blood, cerebrospinal fluid (CSF), extracellular

(interstitial) fluid and the intracellular fluid (cytoplasm). These compartments are dynamic and fluid may move from one compartment to another due to water permeability of the membranes. An example of this is a physiological astrocytic swelling seen after local neuronal activity (57,58). The brain has an especially tight control of fluid movement between blood and the interstitial space due to the Blood-Brain Barrier (BBB). The innermost layer of the BBB is the vascular wall consisting of endothelium, basal laminae, and pericytes embedded in the basal laminae at the capillary level (3). In contrast to other vasculature in other organs, cerebral vessels have tight junctions connecting endothelial cells minimizing paracellular transport (3). In direct connection to the vascular basal lamina is a single layer of astrocytic endfeet, covering the entire vessel providing the outmost border of the brain interstitial space (33). In larger vessels, the pericytes are replaced by smooth muscle covering the endothelium. Another distinction in the anatomy of larger parenchymal vessels is a gap between the vascular wall and the astrocyte endfeet known as the Virchow-Robin space (57,59). This space constitutes a paravascular pathway for CSF circulation in the brain parenchyma (59).

Oedema is the pathological process of tissue swelling due to increased fluid content. There are two requirements for oedema formation. First, There needs to be a driving force moving fluid to the brain parenchyma. The balance of driving forces are best explained by Starling's principle of fluid exchange (58). In short, the sum of osmotic and hydrostatic pressure across the vessel and parenchyma determines the direction of fluid movement. Second is the need for perfusion as more fluid will be required to add mass to the tissue. The need for perfusion is seen in human stroke as oedema is first formed in the, damaged yet perfused, penumbra (60).

Historically, oedema is divided into cytotoxic and vasogenic oedema, however it is becoming increasingly clear that this picture requires some more nuance (58). Cytotoxic, also known as cellular, oedema is caused by metabolic dysfunction resulting in high intracellular osmolarity. The heightened osmolarity will passively draw water into the cell and make it swell. In the brain, astrocytes are the primary drivers of cytotoxic oedema, largely due to the expression of AQP4 (57). AQP4 allows free and rapid passage of water into astrocytes, and is detrimental during development of cytotoxic oedema (57,61). Cytotoxic oedema understood as cellular swelling is in fact not a real form of oedema as there is no mass effect. However, it is a driving force in subsequent forms of oedema adding fluid mass to the tissue (58). Ionic

oedema often follows cytotoxic oedema and is caused by increased transport of water and osmoles across the endothelium (58). This is without any break in the integrity of the BBB.

In contrast, vasogenic oedema is characterized by extracellular fluid accumulation containing plasma proteins (3,58). This is due to a breakdown of the blood-brain barrier and the subsequent leak of exudate in the brain interstitial space. In the previous paragraph, we discussed the deleterious role of AQP4 in intracellular oedema. However, in the case of vasogenic oedema, AQP4 helps clear the extracellular oedema (62). Mechanistically, the breakdown of the BBB may be caused by multiple proteins such as thrombin, VEGF, or MMP9 (63). With sufficient breakdown of the vascular wall, a haemorrhagic transformation may occur with accumulation of blood in the brain parenchyma (58). Estimates show that haemorrhagic conversion happens in 3-40% of ischemic stroke patients, and is associated with risk factors such as hypertension, age, and inflammatory markers in patients (64).

Even small oedemas may impede brain tissue function and cause damage. As the brain is encapsulated in a rigid skull, swelling of the brain tissue will increase the intracranial pressure. If the pressure of the brain parenchyma exceeds the capillary pressure it may close of the local capillaries thus leading to ischemic damage (58). Larger infarctions may produce an oedema of sufficient size to threaten brain herniations. These malignant infarctions occur in 1-10% of ischemic stroke cases and are correlated with considerable mortality (65). Brain herniation most commonly occurs in the following regions; gyrus cinguli being forced under the falx cerebri, herniation across the tentorium cerebelli, and herniation out of the foramen magnum. The latter is considered a life threatening condition due to pressure being applied to the reticular substrate of the medulla oblongata responsible for respiration and cardiovascular regulation. Herniation may cause a temporary loss of function in the region, and in severe cases lead to irreversible tissue damage. Whether herniations occur depends on both the size of the oedema, and the local anatomical considerations. For example, cerebellar infarctions are particularly vulnerable to herniation due to the anatomical constraints of the fossa cranii posterior and tentorium cerebelli. Currently, the treatment of threatening herniation is to make more space by decompressive craniectomy (14). There are no treatments directly modifying the mechanisms behind oedema formation, nor oedema resolution.

1.5 – Innate neuroinflammation and astrogliosis

Inflammation in the brain is an double edged sword and requires strict control. A testament to this is the brains parenchyma's relative immune privilege keeping the circulating immune system at bay (66). This is primarily due to the BBB and humoral factors secreted by astrocytes (66). However, the BBB may be compromised in various brain pathologies, including stroke, leading to the infiltration of leucocytes to the brain parenchyma (67). Neutrophils invade the infarction core as soon as 5 hours after onset of stroke, and will reach a peak after 12 hours (68). Monocytes and macrophages are seen in the infarct core after 3 days taking over the neutrophils, and reach the peak concentration after 7 days (68). In acute injuries, excess neutrophilic infiltration will exacerbate the secondary neuronal loss (68). Counteracting this is the formation of a glial scar surrounding lesions. The glial scar will limit the neutrophils from reaching peri-lesion areas and reduce the neuronal degeneration (69).

Glial cells constitute the innate immune cells of the CNS. Astrocytes and microglia have an particularly important role as first responders to tissue damage (70). Quickly after the onset of ischemic stroke, neurons as well as other cells become necrotic. This initiation of tissue damage leads to the release of factors such as glutamate, ATP and danger-associated molecular patterns (DAMPs) which lead to the activation of local astrocytes and microglia (70). This process of reactive gliosis will further propagate as reactive astrocytes and microglia will secrete cytokines activating and recruiting other dormant glial cells. More recent research eludes that this propagation of gliosis is not only a focal phenomenon, but might affect the whole brain (4).

Reactive astrocytes undergo a number of cellular events in a time pendent manner. First, is the change in protein expression. One of the proteins upregulated is Glial Fibrillary acidic protein (GFAP), an astrocyte specific intermediary filament, which expression peaks 2 days after experimental stroke (71). Reactive astrocytes will also start proliferation, with the peak of proliferation occurring after 4 days (71). The final step of reactive astrogliosis is the migration towards the lesion and formation of a glial scar, which starts to take shape after 6-8 days and continues to mature (71). Parallel to the formation of the glial scar is a change in morphology, where highly reactive astrocytes will align their processes towards the lesion (71). This is often seen as a step in the maturation of the glial scar. Glial scarring is however the extreme outcome of astrogliosis and is usually confined to the area directly bordering a lesion. Areas further away may exhibit lesser degrees of astrogliosis with temporary disruption of homeostatic functions before resolving back to a normal state.

More recently AQP4 has been shown to be involved with the immunological properties of astrocytes. Stab wound experiments to the brain show that mice lacking AQP4 have less upregulation of GFAP and hence less astrogliosis (72). Similarly, MPP+ injections, modelling Parkinson's disease, in the brains of AQP4 deficient mice have less microglial activation (53). AQP4 is also important for migration of reactive astrocytes and the formation of a glial scar as seen in stab wound experiments (29). Previous reports show a depolarization of AQP4 from the perivascular endfeet, as well as an upregulation of AQP4 expression in reactive astrocytes (51). It will therefore be of value to compare the temporal and special regulation of AQP4 in stroke to that of reactive gliosis.

1.6 – Sexual dimorphisms of the brain

There are differences in both anatomy and gene expression between male and female humans as well as lesser vertebrates (73). Great caution must be applied in using these differences to behavioural and cognitive differences as there are many pitfalls in correlation based assumptions. However, it would be negligent to disregard these differences when studying neurological disease. When it comes to gross anatomy, in human but not mice, the mean male brain is 10% larger than female brain, however, this is with a large variation and overlap between genders (73). There are also region specific differences in gray matter volume between human male and females (74). Sexual dimorphism also affects astrocytes and microglia. In a model of experimental stroke, markers of reactive gliosis were more pronounced in male mice (75).

1.7 – Experimental stroke and comparative medicine

Modelling stroke in rodents may be performed in a number of ways, and different methods may be more applicable to research specific areas of stroke pathology. The most common occlusion in human stroke is in the middle cerebral artery (MCA) (76), and this is also reflected in animal models of stroke. Traditionally, proximal middle cerebral artery occlusions (pMCAO) or occlusions of the internal carotid artery have been the main targets for inducing experimental stroke. This may be performed by binding a suture around the artery, or by intravasal blocking (77). pMCAO will produce large infarctions, covering cerebral cortex and striatum, and often allow for removal of the occlusion making them ideal for studying oedema formation and reperfusion injuries (77).

More focal lesions are produced by distal middle cerebral artery occlusions (dMCAO) models of stroke. These are often permanent occlusions that require transcranial surgical access. Clipping, photothrombotic coagulation, and electrocoagulation are all methods to achieve dMCAO (77). Here the infarction is more limited to the cerebral cortex, and the infarct volume reflects human cortical stroke (78). Apart from the artery occluded, it is important to consider the duration of the occlusion. Permanent occlusions, especially in dMCAO, often better reflect human stroke. These models will however have less oedema, and are not suitable for the study of reperfusion injuries. Transient occlusions will vary in severity based on the occlusion time and the time allowed for reperfusion. These may be better for the study of oedema and reperfusion injuries. However, for drug discovery it is recommended to use permanent occlusions as these better reflect the time windows applicable in a clinical setting (79).

Is it possible to compare the human and murine brain? Apart from the obvious differences such as size and gyrification, there are also microscopic differences that need to be accounted for. Of interest is the increased complexity of human astrocytes. The astrocyte to neuron ratio is increased in species of higher cognition. The ratio of *C. elegans* is 0.18, for rats it is 0.4, and for human it is 1.0 in the whole brain and 1.4 in the cortex (30). In addition, the individual human astrocytes is more complex. They are larger, more branched and cover more synapses than mouse astrocytes (30). There is also a subtype of astrocytes, the interlaminar astrocyte, which is specific to primates (30). Despite these differences, both human and mouse astrocytes have the same specialized domains, such as perivascular endfeet, and they both have the same baseline functions including homeostatic functions, signalling, and in reactive astrogliosis.

2 – Methods

2.1 – Search method and criteria

A systematic search was conducted on PubMed to include all papers with the criteria “(stroke) OR (ischemia) AND (AQP4)” in the title, keywords or abstract. The search was conducted on 05. April 2022 yielding 477 papers identified. Prior to the discovery of AQP4, OAPs had been studied in the relation to stroke. These papers were not included in the search as OAPs had not been defined properly yet. Abstracts were screened for the following inclusion criteria in the different categories.

AQP4 in human stroke:

All papers measuring AQP4 protein levels, immunohistochemistry or mRNA levels in humans after stroke were included. This yielded 7 papers from 2003 onwards which were a mix of post mortem histopathological studies, and clinical studies measuring AQP4 levels in blood samples.

AQP4 in experimental stroke in mice:

Inclusion criteria:

1. Species must be *Mus Musculus*, all strains are included
2. Must yield quantitative data on either protein or RNA expression of AQP4
3. Must compare ipsilateral tissue in stroke group to either:
 - a. Contralateral tissue within same animal
 - b. Sham group
4. Must adequately describe experimental occlusion method and the length of occlusion time in cases of temporary occlusion models
5. Occlusion must primarily give hypoxic injury to CNS tissue

Exclusion criteria:

- Is a review article or shows no novel experimental data
- Data is from in-vitro studies

Outcome measure:

- Results from qPCR for AQP4 mRNA expression
- Results from western blotting and immunohistochemistry for AQP4 protein expression
- Results from immunohistochemistry, either qualitative or quantitative, for AQP4 perivascular polarization

For protein analysis 29 papers were identified and included. For mRNA analysis 3 papers were included. These were papers which show experimental data measuring both protein and mRNA levels, and are therefore included in both groups of papers.

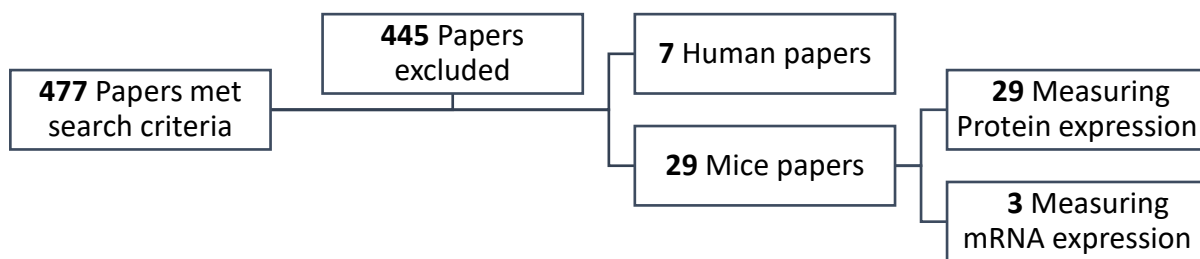


Figure 1: Visualizing the papers considered and included in this review.

2.2 – Comparing quantitative data

Comparing animal experiment can pose a challenge. Experimental conditions, age, sex and strain of animals may all effect the results. However, heterogeneity is a common challenge in human clinical research, and it is often resolved in a satisfactory manner.

For the papers included here regarding experimental stroke in mice, the main concern is the lack reporting of statistical values such as means and standard deviations. It is an unfortunate trend to report significance (p-values) to denote a difference without reporting the magnitude of the difference. Therefore we have had to manually read means of the graphs to get estimates for the fold change between infarct and control samples. This poses an inaccuracy, however, it is still of value to have estimates of the fold change. The changes are denoted with arrows in **table 2-6**, to give a visual estimate of the magnitude of change.

The methods used for post-mortem analysis is also of importance. For protein expression both western blotting and immunohistochemical methods are commonly used. Western blotting is given more weight in the conclusions of this review due to it being less prone to artefacts, and more reliable in quantitatively assessing relative protein amounts and antibody specificity. For the analysis of perivascular versus non-perivascular AQP4 there are two main methods of immunocytochemistry. The most common and readily available is immune staining for light or laser-scanning microscopy. The main advantage of these methods is the availability of the methods. However, the theoretical resolution limit of light microscopy is around 200nm, while the smallest astrocyte endfeet may be as thin as 20nm (33). Therefore, light microscopy cannot differentiate the polarized adluminal pool of AQP4 from any mislocalized abluminal AQP4 in the astrocytic endfeet. To overcome this

limitation, researchers also use immunogold transmission electron microscopy which is able to disseminate these nanoscale differences. Therefore electron microscopy results will be given more weight in the conclusions of this review.

2.3 – Strain, age and sex in animal experiments

Paper	Mice		
	Strain and other info	Gender	Age
Ribeiro et al., 2006) (80)	ICR-CD1	Male	Adult, age not specified
Shin et al., 2011 (81)	C57BL6	Male and female	10-11 weeks
Steiner et al., 2012 (82)	C57BL6	Male	8-12 weeks
Filchenko et al., 2020 (83)	C57BL6J	Male	6 weeks
Zeng et al., 2012 (84)	Strain not specified, WT control to AQP4 KO	Male	12 weeks
Coomber & Gibson, 2010 (85)	C57BL6 Placebo for intervention	Female	Adult, age not specified
Xiong et al., 2014 (86)	C57BL6J	Male	<i>Data lacking</i>
H. Wang et al., 2020 (87)	C57BL6	Male	<i>Data lacking</i>
Guo et al., 2021 (88)	TG backcrossed to B57C6J	Male	8-10 weeks
Frydenlund et al., 2006 (89)	C57BL6	Male	Adult, age not specified
X. Liu et al., 2008 (90)	C57BL6	Male and female	<i>Data lacking</i>
Migliati et al., 2010 (91)	C57BL6	Male	<i>Data lacking</i>
N. Liu et al., 2011 (92)	ICR	Male	8 weeks
Chu et al., 2017 (93)	WT control for TG, strain not specified	Male	12-16 weeks
Tang et al., 2014 (94)	CD1	Male	Adult, age not specified
Lo et al., 2005 (95)	WT control for TG, strain not specified	<i>Data lacking</i>	Adult, age not specified
Y. Wang et al., 2015 (96)	CD1	Male	Adult, age not specified
Nakano et al., 2018 (97)	ddY, vehicle control for intervention	Male	6-8 weeks
Hawkes et al., 2013 (98)	WT control for TG experiment	Male and female	12 months

Yan et al., 2016 (99)	C57BL6	Male	Adult, age not specified
Morrison & Filosa, 2016 (75)	C57BL6/CX3CR1	Heterozygous male and female	6-8 weeks
Mages et al., 2019 (100)	C57BL6J	Male	10 weeks
L. Liu et al., 2020 (101)	C57BL6	Male	10-18 weeks
Cui et al., 2015 (102)	Controls for TG experiment	Male	12-16 weeks
Monai et al., 2019 (103)	C57BL6	Male and female	9 weeks
Sanchez-Bezanilla et al., 2019 (104)	C57BL6	Male	10 weeks
Zhang et al., 2022 (105)	C57BL6	Male	10-12 weeks
Banitalebi et al., 2022 (106)	C57BL6	Male and female	6 weeks
Li et al., 2011 (107)	C57BL6N	Male	10-12 weeks

Table 1: Showing all mouse experiment papers with strain, sexes represented and age. WT – Wild type genetic background, AQP4 KO – genetic knock out lacking AQP4 expression, TG – Transgenic, Vehicle control – Used in intervention studies as a negative control.

Most papers used the C57BL6 or related strains. 11 out of 29 papers used different strains, or did not specify what strain was used. This may be a source of some variability when comparing results from the different studies. However, this may be a minor issue.

There is an obvious preference for the use of male mice in these experiments with 21 out of 29 papers only using male mice. Only 5 papers explicitly stated that they used both male and female mice. This fact does provide a challenge when discussing the results as there are important sexual dimorphisms which may effect out outcome measures. These include a difference in astrogliosis (79) which may effect AQP4 expression.

Age is another important factor to consider as most human strokes affect mature adults and the elderly. To better compare human and mouse we need to consider the developmental milestones in the mouse life cycle. Puberty hits after 6 weeks, sexual maturity and early adulthood at age of 8-12 weeks (108). In adulthood, 2.6 days for a mouse is equivalent to one year of human life (108), and the life expectancy of a laboratory mouse is around 2 years. In table 1 we see that most papers have conducted their experiments on mice in the 8-16 week range. This is equivalent to early to middle adulthood. Disappointingly, 11 papers did not specify age of the animals at the start of the experiments.

3 – Results

3.1 – AQP4 in Human stroke

Paper	Method (N)	Result
Aoki et al., 2003 (109)	Post mortem qualitative IHC	↑ AQP4 in glial scar ↑ AQP4 in subpial endfeet in Cx distal to lesion
Satoh et al., 2007 (110)	Post mortem qualitative IHC	↑↑ AQP4 in glial scar ↑ AQP4 proximal to lesion
Mogoanta et al., 2014 (111)	2-63d post mortem qualitative IHC	↑ AQP4 in glial scar ↑ AQP4 colocalized with GLT-1
Stokum et al., 2015 (112)	Post mortem qualitative IHC	↓ perivascular AQP4 in Cx ↑ neuropil AQP4 in WM
Roşu et al., 2019 (113)	Post mortem qualitative IHC	↑ AQP4 in glial scar ↑ neuropil AQP4 in proximal peritonsillar Cx ↑ neuropil AQP4 in WM
Kleffner et al., 2008 (114)	Genetic sequencing	One AQP4 gene polymorphism associated with severe brain oedema
Marazuela et al., 2021 (115)	Clinical blood sample analysis	Plasma AQP4 level negatively correlate with NIHSS at admission Plasma AQP4 at admission correlates positively to better outcome at 48h Plasma AQP4 is higher 2h post admission than in controls

Table 2: Papers regarding AQP4 in human stroke. ICH – Immunohistochemistry, arrows indicate qualitative changes.

Five out of seven papers included where pathohistological studies examining AQP4 protein expression in post mortem samples. These show the end result of AQP4 disruption and are qualitative in nature. Across multiple studies it is shown that AQP4 is upregulated in the glial scar (109–111,116). In addition, some studies show a increase in AQP4 in the border zone beyond the glial scar (110,112). In the border, there is also a relative loss of perivascular AQP4 compared to neuropil AQP4 (112,116). Two studies also show a increase in neuropil AQP4 in the white matter (112,116), while one study shows a increased colocalization of AQP4 to GLT-1 which is a astrocytic glutamate transporter(111).

One paper was focused on finding AQP4 polymorphisms which potentially could explain variation in oedema formation. The result from this study was the identification of a single polymorphism which was significantly correlated with severe brain oedema (114).

Lastly, a clinical trial was conducted comparing clinical stroke measures to serum AQP4 levels. Interestingly, high serum AQP4 is correlated with lower NIHSS at admission, and serum AQP4 was shown to be prospective for the 48 hour post-admission outcome (115).

3.2 – AQP4 Protein expression in experimental stroke

Paper	Stroke model			Protein analysis	
	Ischemic region	Artery	occlusion time	Method (N)	Results
Ribeiro et al., 2006 (80)	striatum	proximal MCA	30 min	IHC (3-6)	<p>1h ipsi vs contra: ↑ AQP4 in infarct border ↑ AQP4 in infarct Core</p> <p>6h ipsi vs contra: ~ AQP4 in infarct border ~ AQP4 in infarct core</p> <p>24h ipsi vs contra: ~ AQP4 in infarct border ~ AQP4 in infarct core</p> <p>48h ipsi vs contra: ↑ AQP4 in infarct border ~ AQP4 in infarct core</p> <p>7d ipsi vs contra: ~ AQP4 in infarct border ~ AQP4 in infarct core</p>
Shin et al., 2011 (81)	Striatum and cortex	Proximal MCA	30 min	WB (3-4)	<p>Control (no operation): ~ AQP4 in male vs female</p> <p>6h vs control: ~ AQP4 in male infarct core (Cx) ~ AQP4 in female infarct core (Cx) ~ AQP4 in male vs female infarct</p> <p>24h vs control: ↓ AQP4 in male infarct core (Cx) ↓ AQP4 in female infarct core (Cx) ↓ AQP4 in male vs female infarct</p> <p>72h vs control:</p>

					<p>↓↓ AQP4 in male infarct core (Cx) ↓ AQP4 in female infarct core (Cx) ↓↓ AQP4 in male vs female infarct</p>
Steiner et al., 2012 (82)	Striatum	Proximal MCA	30 min	WB (3-4)	<p>12h vs sham: ~ AQP4 in infarct border (Cx) ~ AQP4 in infarct core (St)</p> <p>24h vs sham: ~ AQP4 in infarct border (Cx) ~ AQP4 in infarct core (St)</p> <p>48h vs sham: ~ AQP4 in infarct border (Cx) ~ AQP4 in infarct core (St)</p>
Filchenko et al., 2020 (83)	Striatum and cortex	Proximal MCA	35 min	IHC (3)	<p>72h vs sham: ↑↑↑ Perivascular AQP4 length in ipsi (Cx) ↑ Perivascular AQP4 length in contra (Cx)</p> <p>↑ AQP4 density in ipsi (Cx) ~ AQP4 density in contra (Cx)</p> <p>↑ AQP4 coverage in ipsi (Cx) ~ AQP4 coverage in contra (Cx)</p>
Zeng et al., 2012 (84)	Striatum and cortex	Proximal MCA	40 min	WB (?)	<p>24h vs contra: ↓ AQP4 in ipsi (Cx)</p> <p>72h ipsi vs contra: ↑ AQP4 in ipsi (Cx)</p>
Coomber & Gibson, 2010 (85)	Striatum and cortex	Proximal MCA	60 min	WB (7)	<p>48h vs sham: ~ AQP4 in ipsi hemisphere</p>
Xiong et al., 2014 (86)	Striatum and cortex	Proximal MCA	60 min	WB (?)	<p>48h vs sham: ↑↑ AQP4 in penumbra (Cx)</p>
H. Wang et al., 2020 (87)	Striatum and cortex	Proximal MCA	60 min	WB (4)	<p>6h vs sham: ↑↑ AQP4 in ipsi hemisphere</p> <p>24h vs sham: ↑↑↑ AQP4 in ipsi hemisphere</p> <p>72h vs sham: ↑↑ AQP4 in ipsi hemisphere</p> <p>5d vs sham:</p>

					<p>↑↑ AQP4 in ipsi hemisphere</p> <p>7d vs sham: ~ AQP4 in ipsi hemisphere</p>
Guo et al., 2021 (88)		Proximal MCA	60 min	WB (8)	<p>24h vs sham: ↑↑ AQP4 in stroke (region not specified)</p>
Frydenlund et al., 2006 (89)	Striatum and cortex	Proximal MCA	90 min	Immunogold EM (2-4)	<p>12h vs control: ~ Perivascular AQP4 in infarct border ~ Perivascular AQP4 in infarct core (St) ↓ Perivascular AQP4 in infarct core (Cx)</p> <p>24h vs control: ↑ Perivascular AQP4 in infarct border ↓ Perivascular AQP4 in infarct core (St) ↓ Perivascular AQP4 in infarct core (Cx)</p> <p>48h vs control: ~ Perivascular AQP4 in infarct border ↓ Perivascular AQP4 in infarct core (St) ↓ Perivascular AQP4 in infarct core (Cx)</p> <p>72h vs control: ~ Perivascular AQP4 in infarct border ↓ Perivascular AQP4 in infarct core (St) ↓ Perivascular AQP4 in infarct core (Cx)</p>
X. Liu et al., 2008 (90)	Striatum and cortex	Proximal MCA	90 min	WB (7)	<p>72h ipsi vs contra: ↓↓ AQP4 in ipsi (Cx) (male and female) ~ AQP4 in male vs female infarct</p>
Migliati et al., 2010 (91)	Striatum and cortex	Proximal MCA	90 min	WB (4)	<p>48h vs sham: ~ AQP4 in infarct core (Cx)</p>
N. Liu et al., 2011 (92)	Striatum and cortex	Proximal MCA	90 min	WB (?)	<p>48h vs sham: ↑↑ AQP4 in ipsi hemisphere</p>
Chu et al., 2017 (93)	Striatum and cortex	Proximal MCA	90 min	IHC (6) and WB (6)	<p>Qualitative IHC: ↓ perivascular AQP4 in infarct border</p> <p>WB vs sham: 24h: ↑↑ AQP4 in infarct core (Cx) 72h: ↑↑↑ AQP4 in infarct core (Cx) 7d: ↑↑↑ AQP4 in infarct core (Cx)</p>
Tang et al., 2014 (94)	Striatum and cortex	Proximal MCA	90 min	WB (6)	<p>24h vs sham: ~ AQP4 in stroke (region not specified)</p>

					72h vs sham: ↑↑ AQP4 in stroke (region not specified)
Lo et al., 2005 (95)	Striatum and cortex	proximal MCA	120 min	WB (3-5)	22h vs sham: ~ AQP4 in ipsi hemisphere
Y. Wang et al., 2015 (96)	Striatum and cortex	Proximal MCA	180 min	WB (3)	24h vs sham: ↑ AQP4 in ipsi hemisphere 72h vs sham: ↑↑ AQP4 in ipsi hemisphere
Nakano et al., 2018 (97)	Striatum and cortex	Proximal MCA	240 min	WB (6)	48h vs sham: ↑ AQP4 in infarct core (St)
Hawkes et al., 2013 (98)	Striatum and cortex	Proximal MCA	Permanent	IF (6)	24h vs contra: ↓↓ AQP4 in infarct core (Cx)
Yan et al., 2016 (99)	Striatum and cortex	Proximal MCA	Permanent	WB (4)	2h vs sham: ~ AQP4 in infarct border 6h vs sham: ↑ AQP4 in infarct border 24h vs sham: ↑ AQP4 in infarct border 48h vs sham: ↑ AQP4 in infarct border
Morrison & Filosa, 2016 (75)	Striatum and cortex	Proximal MCA	Permanent	IHC (6-7)	1h vs sham: ↑↑ Neuropil AQP4 Male border (Cx) ~ Neuropil AQP4 in Female border (Cx) ~ Neuropil AQP4 in Male distal (Cx) ~ Neuropil AQP4 in Female distal (Cx)
Mages et al., 2019 (100)	Striatum and cortex	Proximal MCA	Permanent	IHC (6)	4h vs contra: ~ AQP4 in infarct core (Cx) ~ AQP4 in infarct border (Cx) ~ AQP4 in infarct core (St) ~ AQP4 in infarct border (St) ↑ AQP4 in core (Cx) vs core (St) ↑ AQP4 in border (Cx) vs core (St) 24h ipsi vs contra: ~ AQP4 in infarct core (Cx) ~ AQP4 in infarct border (Cx) ~ AQP4 in infarct core (St) ~ AQP4 in infarct border (St) ↑ AQP4 in core (Cx) vs core (St)

					↑ AQP4 in border (Cx) vs core (St)
L. Liu et al., 2020 (101)	Striatum and cortex	a. carotis communis	Permanent	IHC (4-5)	24h vs sham: ↑↑ AQP4 in CA1 (Hc)

Table 3: Protein levels in proximal MCA occlusions. MCA – Middle cerebral artery, ICH – Immunohistochemistry, WB – Western blot (SDS-PAGE), ? – value not provided, ↑ 1-2 fold increase, ↑↑ 2-4 fold increase, ↑↑↑ more than 4 fold increase, ~ no significant difference, ↓ up to 0.5 fold decrease, ↓↓ more than 0.5 fold decrease, ↓↓↓ Loss of detectable signal. Ipsi – Ipsilateral to infarct, contra – contralateral to infarct, sham – mice operated without occlusion of artery, (Cx) Cerebral cortex, (St) Striatum, (Hc) Hippocampus, infarct core – the central area of infarction, infarct border – non-ischemic tissue directly surrounding the infarct core.

The pMCAO models of stroke produce infarctions in the striatum and, if the occlusion-time is long enough, the cortex directly above. These infarctions may be severe and effect large portions of the ipsilateral hemisphere directly. Most of the studies included examine AQP4 expression within 48 hours of occlusion, while the longest timepoint is at 7 days.

First we will consider the changes in AQP4 protein expression. Starting with the earliest timepoints we have 3 papers describing AQP4 expression after 1 hour (75,80) and 2 hours (99) after ischemia. First, after 30 min transient occlusion Ribeiro et. al. show a increase in total AQP4 in both the infarct core and border (80). In permanent occlusions, Yan et al. shows no difference in AQP4 expression (99), while Morrison and Filosa show a specific increase in neuropil AQP4 in male, but not female, infarct border (75). In the 4 to 6 hour timeframe, the results are still split with two studies showing an increase in AQP4 expression, both in infarct border (99) and the ipsilateral hemisphere (87). While three studies show no significant difference (80,81,100). Curiously, Mages et al. does show that while AQP4 levels does not change in infarct regions compared to contralateral hemisphere, there is an relative increase in ischemic cortex compared to ischemic striatum (100). One study also shows a upregulation of AQP4 in the CA1 of the hippocampus 24 hours after pMCAO (101).

Moving on to the 12 and 24 hour marks the changes in AQP4 protein levels and perivascular polarization become more clear. First, 12 hours after stroke Steiner et al. show no difference in AQP4 protein levels in infarct core and border (82). After 24 hours a general upregulation of AQP4 occurs in the ipsilateral hemisphere (87,96). This is despite a relative

loss of AQP4 in the cortex (81,84,98). Looking at the infarct core two papers show a loss of AQP4 (81,98), three papers show no change (80,82,100), and one shows a upregulation of AQP4 (102). In the border, Yan et al. showed a increase in AQP4 using a permanent occlusion (99), while Ribeiro et al. using a 30 minute occlusion and reperfusion model showed no difference (80).

2 days after infarction Liu et al. show a increase in AQP4 in the ipsilateral hemisphere (92), while Coomber and Gibson show no difference (85). Nakanao et al. show that the striatum infarct core has increased AQP4 expression in a 240 minute long occlusion (97), while Migliati et al. show no difference in cortical infarct core (91). In shorter occlusions (30 minutes) Ribeiro et al. and Steiner et al. show no difference in infarct core (80,82). There is an increase of AQP4 in the infarct border in both 30 minute and permanent occlusions (80,99).

Day 3 post infarction shows the same pattern as day 2. There is an upregulation of AQP4 when looking at the ipsilateral hemisphere (83,87,94,96). When looking specifically at the infarct core there is conflicting results. Chu et al. report a increase in AQP4 (93), while shin et al. report a loss of AQP4 with a higher loss in male versus female mice (81). There are also conflicting results in the longer time points. H. Wang et al. show an increase in AQP4 in the ipsilateral hemisphere after 5 days, which normalized after 7 days (87). However, Chu et al. does show an increase in AQP4 expression after 7 days (93). Lastly, Ribeiro et al. show no changes in the infarct core or border after 7 days (80).

Frydenlund et al. have examined the perivascular polarization of AQP4 in both infarct core and border at different time points after infarction. In the ischemic cortex, a loss of perivascular AQP4 can be seen as early as 6 hours after infarct, and it reaches its lowest value after 24 hours. In the striatum part of the infarct core, a loss of AQP4 polarity can be seen after 24 hours, equivalent to that in the infarct cortex. The infarct border however has a transient drop of perivascular AQP4 at 6 hours. This is followed by an increase in perivascular AQP4 after 24 hours which normalizes after 48 hours (89). Chu et al. does show that there is a loss of perivascular AQP4 in the border after 24 hours, this however is not quantified (93). At 72 hour after stroke Filchenko et al. report an increase in perivascular AQP4 both in the ipsilateral and contralateral hemispheres (83), while Frydenlund et al. show an loss in the infarct core, and normalization in the infarct border (89).

Paper	Stroke model			Protein analysis	
	Ischemic region	Artery	occlusion time	Method (N)	Results
Cui et al., 2015 (102)	Cortex	Distal MCA	Permanent	IF (?) and WB (4)	7d vs sham: ↓ AQP4 in stroke (both IHC and WB)
Monai et al., 2019 (103)	Cortex	Distal MCA	Permanent, phototrombotic	IF (6) and WB (4)	1h vs contra: ↑ AQP4 in infarct core (Cx) 2h vs contra: ↓ AQP4 in infarct core (Cx) 3h vs contra: ↓↓ AQP4 in infarct core (Cx) 24h vs contra: ↓↓ AQP4 in infarct core (Cx)
Sanchez-Bezanilla et al., 2019 (104)	Cortex	Distal MCA	Permanent, phototrombotic	IF (10) and WB (7)	14d vs sham: ↓ AQP4 in infarct border (Cx) ~ AQP4 in thalamus ~ AQP4 in hippocampus ↓ Perivascular AQP4 in infarct border ↓ Perivascular AQP4 in thalamus ~ Perivascular AQP4 in hippocampus
Zhang et al., 2022 (105)	Cortex	Distal MCA	Permanent, phototrombotic	IF (N unknown)	2.5h vs sham: ~ AQP4 in ipsi (Cx) ~ AQP4 in ipsi (St) ↓ Polarized AQP4 in ipsi (Cx) ↓ Polarized AQP4 in ipsi (St) ↓ of AQP4 in ipsi ependymal cells
Banitalebi et al., 2022 (106)	Cortex	Distal MCA	Permanent, electrocoagulation	BN (6) and WB (6)	7d vs contra: ↓ OAPs in infarct core and border ~ Total AQP4 in infarct core and border ~ M23-AQP4 in infarct core and border ↓ M1-AQP4 in infarct core and border ↓ AQP4ex in infarct core and border

Table 4: Protein expression in distal MCA occlusion. MCA – Middle cerebral artery, ICH – Immunohistochemistry, WB – Western blot (SDS-PAGE), ? – value not provided, ↑ 1-2 fold increase, ↑↑ 2-4 fold increase, ↑↑↑ more than 4 fold increase, ~ no significant difference, ↓ up to 0.5 fold decrease, ↓↓ more than 0.5 fold decrease, ↓↓↓ Loss of detectable signal. Ipsi – Ipsilateral to infarct, contra – contralateral to infarct, sham – mice operated without occlusion

of artery, (Cx) Cerebral cortex, (St) Striatum, (Hc) Hippocampus, infarct core – the central area of infarction, infarct border – non-ischemic tissue directly surrounding the infarct core.

All papers using a dMCAO performed permanent occlusions (**Table 4**). This yields results that are not compounded by reperfusion injuries, and all infarctions are limited to the cortex. Monai et al. shows a transient upregulation of AQP4 in the infarct core 1 hour after occlusion which turns into a loss of AQP4 at the 2 and 3 hour as well as the 24 hour time points (103). Zhang et al. report that there is no loss of AQP4 expression in the ipsilateral cortex nor striatum, however there is a loss of perivascular AQP4 polarization 2.5 hours after occlusion (105). Cui et al. show a loss of AQP4 7 days after occlusion (102). In our own research we found no difference in total AQP4 7 days after occlusion. However, we did observe a selective loss of the isoforms AQP4ex and M1-AQP4 in the infarct core and border. This was accompanied by a loss of perivascular AQP4 and disruption of OAPs in the same region (106). Lastly, Sanchez-Bezanilla et al. show a reduction of AQP4 expression and perivascular AQP4 at the infarct border 14 days post occlusion (104).

Paper	Stroke model			Protein analysis	
	Ischemic region	Artery	occlusion time	Method (N)	Results
Li et al., 2011 (107)	Retina	a. Carotis interna	120 min	IHC (?)	22h vs sham: ↑↑ AQP4 in ipsi

Table 5: Protein expression in retinal ischemia. ICH – Immunohistochemistry, ? – value not provided, ↑ 1-2 fold increase, ↑↑ 2-4 fold increase, ↑↑↑ more than 4 fold increase, ~ no significant difference, ↓ up to 0.5 fold decrease, ↓↓ more than 0.5 fold decrease, ↓↓↓ Loss of detectable signal. Ipsi – Ipsilateral to infarct, contra – contralateral to infarct, sham – mice operated without occlusion of artery.

Li et al. explored the consequences of retinal ischemia on AQP4 expression and reported a increase of AQP4 in the ischemic retina 22 hours after occlusion (107) (**Table 5**).

3.3 – AQP4 mRNA expression in experimental stroke

Paper	Stroke model			mRNA analysis	
	Ischemic region	Artery	occlusion time	Method (N)	Results
Shin et al., 2011 (81)	Striatum and cortex	Proximal MCA	30 min	qPCR (4)	Control cx: ~ AQP4-mRNA in male vs female 6h vs control: ~ AQP4-mRNA in male core (Cx) ~ AQP4-mRNA in female core (Cx) ~ AQP4-mRNA in male vs female 24h vs control ↓↓ AQP4-mRNA in male core (Cx) ↓ AQP4-mRNA in female core (Cx) ~ AQP4-mRNA in male vs female core (cx) 72h vs control ↓↓ AQP4-mRNA in male core (Cx) ↓↓ AQP4-mRNA in female core (Cx) ~ AQP4-mRNA in male vs female core (cx)
Tang et al., 2014 (94)	Striatum and cortex	Proximal MCA	90 min	qPCR (6-9)	24h vs sham: ~ AQP4-mRNA in ipsi 72h vs sham: ↑↑↑ AQP4-mRNA in ipsi
Y. Wang et al., 2015 (96)	Striatum and cortex	Proximal MCA	180 min	qPCR (3)	24d vs sham: ↑↑ AQP4-mRNA in ipsi hemisphere 72d vs sham: ↑↑↑ AQP4-mRNA in ipsi

Table 6: mRNA expression in experimental stroke. MCA – Middle cerebral artery, ICH – Immunohistochemistry, WB – Western blot (SDS-PAGE), ? – value not provided, ↑ 1-2 fold increase, ↑↑ 2-4 fold increase, ↑↑↑ more than 4 fold increase, ~ no significant difference, ↓ up to 0.5 fold decrease, ↓↓ more than 0.5 fold decrease, ↓↓↓ Loss of detectable signal. Ipsi – Ipsilateral to infarct, contra – contralateral to infarct, sham – sham-operated mice, (Cx) Cerebral cortex, (St) Striatum, (Hc) Hippocampus, infarct core – the central area of infarction, infarct border – non-ischemic tissue directly surrounding the infarct core.

All studies looking at mRNA levels are done with a pMCAO model, with occlusion times varying between 30-180 minutes (**Table 6**). Shin et al. report a loss of AQP4-mRNA in the infarct core which starts 24 hours after infarction and persist at least until 72 hours after infarction (81). When looking at the ipsilateral hemisphere as a whole, Y. Wang et al. show a increase in AQP4-mRNA 24 hours after occlusion. This is contradicted by Tang et al. which shows no difference. Both studies however show an increase in AQP4-mRNA after 72 hours (94,96).

4 – Discussion

4.1 – AQP4 in stroke research

AQP4 was first discovered by its mRNA expression in the brain in 1994 (117,118), and shortly after its importance in water homeostasis in the CNS was proven using transgenic mice lacking the water channel (119). The discovery of a molecular pathway for water homeostasis prompted scientists to explore how AQP4 may relate to oedema and vascular illnesses such as stroke. In 2000 Manly et al. Showed the protective effects of genetically deleting AQP4 in mice undergoing both water intoxication and experimental stroke (120). Following this, Amiry-Moghaddam et al. showed that mice lacking alpha-syntrophin, disrupting the perivascular polarization of AQP4, had smaller infarct volumes and less oedema than wild type mice after experimental stroke (121). Since then, it has become apparent that AQP4 plays a central role in stroke pathophysiology. However, the knowledge on regulation of AQP4 itself after stroke has been elusive due to conflicting results which we will now attempt to clarify.

Summarizing the papers on experimental stroke in mice shows the following (**Table 3-4**). AQP4 is upregulated in the infarction 1 hour after ischemia, likely in the neuropil (80,103). In the following hours there is disagreement between papers using distal and proximal occlusions. 2-4 hours after dMCAO there is a loss of AQP4 expression and perivascular polarization (103,105), while in pMCAO studies either show no difference or increased expression of AQP4 (99,100). The results at 6 to 24 hours post occlusion are inconclusive with studies showing an increase (87,88,93,96,99,101), decrease (81,84,103) or no change in total AQP4 expression (80,82,94,95,100). The 6 hour mark trends more towards

a loss of total AQP4 expression, while 12-24 hours post occlusion are more inconclusive. However, the perivascular pool of AQP4 is at its lowest 24h after stroke (89). The same pattern with conflicting results continue 2 days post occlusion with studies showing either no change in AQP4 expression in the infarct border (82,85,89) or an increased expression in the same region (80,86). 3 days after pMCAO there is an upregulation of AQP4 mRNA (94,96), and this is followed by an increase in AQP4 expression when examining the entire ipsilateral hemisphere (84,87,94,96). In contrast, 7 days after dMCAO results show either loss or no difference in AQP4 expression (80,87,106). There is also seen a specific loss of the isoforms AQP4ex and M1-AQP4 as well as a loss of perivascular polarization in the infarct border (106). The loss of AQP4 expression and perivascular polarization is also seen 14 days after occlusion in the infarct border (104). There are no studies looking at timepoint further than 14 days which limits our knowledge of AQP4 expression in the chronic stages of stroke pathology. The variation seen, especially in pMCAO, can best be explained by the fact that most papers used a transient occlusion with different occlusion times. Therefore, the extent of hypoxic injury, as well as the following reperfusion injury, will vary and potentially produce different cellular responses.

Regarding the research on human samples we see a similar trend for the localization of AQP4 (**Table 2**). The post mortem samples showing AQP4 expression in the chronic stages after stroke show a upregulation of AQP4 as well as a disruption of its perivascular polarization in the glial scar (109–111,116). This correlates well with data from experimental stroke in mice having disrupted polarization. Of great interest is also the use of AQP4 in blood samples as a biomarker for stroke (115), similar to how troponins are used for cardiac infarcts.

4.2 – The relation of AQP4 expression to Oedema and astrogliosis

It is important to understand the temporal changes in AQP4 expression in the context of the stages of oedema formation. As oedema formation requires perfusion of the brain, more weight is given to the transient occlusion models of experimental stroke when discussing the involvement of AQP4 in oedema. Intracellular oedema are the sole forms of oedema in the first hours after ischemia (3). While extracellular oedema formation may start 6 hours after ischemia, and reaches a peak after 2 days (3). It is important to distinguish these as AQP4 is shown to have promote intracellular oedema formation, while reducing

extracellular oedema. In the present review we see a general trend for downregulation of AQP4 before the 6 hour mark, which can be seen as a compensatory mechanism attempting to attenuate intracellular oedema formation. As time progresses, the transient loss of AQP4 turns into an increase in AQP4 expression, however with a loss of polarity in the infarct border region, which aids in clearance of extracellular oedema.

Reactive astrogliosis, as characterized by increased GFAP expression, is seen minutes to hours after stroke. While the earliest timepoint on AQP4 expression after experimental stroke are on an hourly basis, making it difficult to assess the temporal relations to GFAP expression. Thus, an in-vivo study with high temporal resolution in the first hours after ischemia is needed to determine if AQP4 disruption is a prerequisite or a result of reactive astrogliosis. However, the beginning glial scar can be seen after 6-8 days, and is seen by the characteristic morphology of reactive astrocytes with elongated processes towards the lesion (71). Since AQP4 is shown to be important for cellular migration (29), it becomes especially important to see the changes in expression and polarization in the infarct border. In the infarct border there is a partial loss of perivascular AQP4, with a complete loss in the beginning glial scar 7 days after dMCAO. The loss of perivascular AQP4 continues at least to 14 days post occlusion. AQP4 protein expression is upregulated at 3-5 days after occlusion as previously stated, however, at 7 days it is either normalized or with a slight loss, and 14 days post occlusion there is a loss of AQP4 expression. Human histopathological studies do confirm the loss of perivascular AQP4. Interestingly, they do also uniformly report an increase in AQP4 expression in the glial scar. This may be seen as a step further in the maturation of the glial scar, and potentially act as an adhesion molecule as proposed by Engel et al. (26).

4.3 – Plausible mechanisms of AQP4 disruption

The anchoring of AQP4 can be summarized to be dependent on three factors: the basal laminae surrounding vessels, the dystrophin associated complex, and the isoform AQP4ex. Laminin and Agrin are components of the vascular basal laminae known to anchor the DAPC through dystroglycan (38). And the DAPC connects to AQP4 through α -syntrophin to the perivascular membrane (38). The last factor necessary for perivascular polarization is AQP4ex (41). The mechanism behind AQP4ex mediated anchoring is yet unknown; however, a recent study does show that the extended c-terminal is constitutively phosphorylated at the perivascular domain (122). These post-translational modifications are

prime candidates for exploring the mechanisms behind AQP4 mislocalization which occurs within hours after ischemia.

Reactive astrocytes and activated pericytes are known to release Matrix Metalloproteases (MMPs) which in turn break down the vascular basal laminae (123,124). Thus the loss of Laminin and Agrin may be an mechanism behind the loss of perivascular anchoring of DAPC and thus AQP4. Counteracting this notion is a study by Frydenlund et al. (89) showing that Dp71 and α -syntrophin (members of the DAPC) preserve their perivascular polarization, while perivascular AQP4 is lost after transient pMCAO. Lastly, our own research show a loss of AQP4ex as well as OAPs in the beginning glial scar (106). This is measured 7 days post infarction, and thus cannot be used to decisively state the mechanism behind the early loss of perivascular AQP4. However, it provides possible avenues to explore in future research as it is now known that AQP4ex is susceptible to post-translational modifications.

4.4 – Shortcomings of experimental stroke research

The studies included with experimental stroke research all use a decently young mouse population. The age range was typically 11-16 weeks which corresponds to early to middle adulthood. Human stroke is known to be an illness of older individuals, usually with comorbidities such as hypertension, atherosclerosis or diabetes. This age and health discrepancy between mouse and human stroke is put forward by Lourbopoulos et al. as one of the main reasons behind the “translational block” in stroke research (56). Another factor to consider is the lack of gender diversity in the papers included. Only 5 out of 29 papers used mice of both genders for their experiments, thus reducing the overall ability to generalize the results for both genders. As a final point, the experimental stroke papers all have short timeframes. The longest examined endpoint was after 14 days, and it is becoming increasingly important to understand the sub-acute and chronic phases of stroke pathophysiology.

5 – Conclusion

The expression and perivascular polarization of AQP4 is described best in the first hours after experimental stroke, and at 7 day post occlusion. The studies looking at 6 to 48

hours after stroke contradict each other, making it difficult to extrapolate. Data from transient MCAO show changes in AQP4 expression to be countermeasures to oedema formation and aid in resolution in the first days after occlusion. Data from experimental stroke also show an loss of perivascular AQP4 as well as a possible loss of total AQP4 in the infarct border one week after occlusion. This is in line with the hypothesis that AQP4 disruption may be important for astrocyte migration and glial scar formation. Also supporting this notion is human pathohistological studies showing a loss of perivascular AQP4 polarization while there is an increase of AQP4 in other membrane domains in the glial scar specifically. These observations are done post-mortem and thus show the chronic phase of stroke. Here it is plausible that AQP4 acts as an adhesion molecule between glial scar forming astrocytes.

References

1. Grysiewicz RA, Thomas K, Pandey DK. Epidemiology of Ischemic and Hemorrhagic Stroke: Incidence, Prevalence, Mortality, and Risk Factors. *Neurol Clin.* 2008 Nov 1;26(4):871–95.
2. Saini V, Guada L, Yavagal DR. Global Epidemiology of Stroke and Access to Acute Ischemic Stroke Interventions. *Neurology.* 2021 Nov 16;97(20 Supplement 2):S6–16.
3. Chen S, Shao L, Ma L. Cerebral Edema Formation After Stroke: Emphasis on Blood–Brain Barrier and the Lymphatic Drainage System of the Brain. *Front Cell Neurosci* [Internet]. 2021 [cited 2022 Jul 27];15. Available from: <https://www.frontiersin.org/articles/10.3389/fncel.2021.716825>
4. Shi K, Tian DC, Li ZG, Ducruet AF, Lawton MT, Shi FD. Global brain inflammation in stroke. *Lancet Neurol.* 2019 Nov 1;18(11):1058–66.
5. Meng L, Hou W, Chui J, Han R, Gelb AW. Cardiac Output and Cerebral Blood Flow: The Integrated Regulation of Brain Perfusion in Adult Humans. *Anesthesiology.* 2015 Nov 1;123(5):1198–208.
6. Ermine CM, Bivard A, Parsons MW, Baron JC. The ischemic penumbra: From concept to reality. *Int J Stroke.* 2021 Jul 1;16(5):497–509.
7. Kasner SE. Clinical interpretation and use of stroke scales. *Lancet Neurol.* 2006 Jul;5(7):603–12.
8. Desai SM, Rocha M, Jovin TG, Jadhav AP. High Variability in Neuronal Loss. *Stroke.* 2019 Jan;50(1):34–7.

9. Powers WJ, Rabinstein AA, Ackerson T, Adeoye OM, Bambakidis NC, Becker K, et al. 2018 Guidelines for the Early Management of Patients With Acute Ischemic Stroke: A Guideline for Healthcare Professionals From the American Heart Association/American Stroke Association. *Stroke*. 2018 Mar;49(3):e46–99.
10. Mokin M, Ansari SA, McTaggart RA, Bulsara KR, Goyal M, Chen M, et al. Indications for thrombectomy in acute ischemic stroke from emergent large vessel occlusion (ELVO): report of the SNIS Standards and Guidelines Committee. *J NeuroInterventional Surg*. 2019 Mar 1;11(3):215–20.
11. Sun MS, Jin H, Sun X, Huang S, Zhang FL, Guo ZN, et al. Free Radical Damage in Ischemia-Reperfusion Injury: An Obstacle in Acute Ischemic Stroke after Revascularization Therapy. *Oxid Med Cell Longev*. 2018 Jan 31;2018:e3804979.
12. Thorén M, Azevedo E, Dawson J, Egidio JA, Falcou A, Ford GA, et al. Predictors for Cerebral Edema in Acute Ischemic Stroke Treated With Intravenous Thrombolysis. *Stroke*. 2017 Sep;48(9):2464–71.
13. Dostovic Z, Dostovic E, Smajlovic D, Ibrahimagic OC, Avdic L. Brain Edema After Ischaemic Stroke. *Med Arch*. 2016 Oct;70(5):339–41.
14. Pallesen LP, Barlinn K, Puetz V. Role of Decompressive Craniectomy in Ischemic Stroke. *Front Neurol [Internet]*. 2019 [cited 2022 Jul 15];9. Available from: <https://www.frontiersin.org/articles/10.3389/fneur.2018.01119>
15. Sandercock PA, Soane T. Corticosteroids for acute ischaemic stroke. *Cochrane Database Syst Rev*. 2011 Sep 7;2011(9):CD000064.
16. Finn RN, Cerdà J. Evolution and Functional Diversity of Aquaporins. *Biol Bull*. 2015 Aug;229(1):6–23.
17. Agre P. The 2009 Lindau Nobel Laureate Meeting: Peter Agre, Chemistry 2003. *J Vis Exp JoVE*. 2009 Dec 9;(34):1565.
18. Preston GM, Carroll TP, Guggino WB, Agre P. Appearance of Water Channels in *Xenopus* Oocytes Expressing Red Cell CHIP28 Protein. *Science*. 1992 Apr 17;256(5055):385–7.
19. Ishibashi K, Tanaka Y, Morishita Y. The role of mammalian superaquaporins inside the cell. *Biochim Biophys Acta BBA - Gen Subj*. 2014 May 1;1840(5):1507–12.
20. Amiry-Moghaddam M, Ottersen OP. The molecular basis of water transport in the brain. *Nat Rev Neurosci*. 2003 Dec;4(12):991–1001.
21. Ho JD, Yeh R, Sandstrom A, Chorny I, Harries WEC, Robbins RA, et al. Crystal structure of human aquaporin 4 at 1.8 Å and its mechanism of conductance. *Proc Natl Acad Sci U S A*. 2009 May 5;106(18):7437–42.
22. Wolburg H, Wolburg-Buchholz K, Fallier-Becker P, Noell S, Mack AF. Chapter one - Structure and Functions of Aquaporin-4-Based Orthogonal Arrays of Particles. In: Jeon KW, editor. *International Review of Cell and Molecular Biology [Internet]*.

- Academic Press; 2011 [cited 2022 Jul 31]. p. 1–41. Available from:
<https://www.sciencedirect.com/science/article/pii/B9780123860439000013>
23. Jin BJ, Rossi A, Verkman AS. Model of Aquaporin-4 Supramolecular Assembly in Orthogonal Arrays Based on Heterotetrameric Association of M1-M23 Isoforms. *Biophys J*. 2011 Jun 22;100(12):2936–45.
 24. Lu M, Lee MD, Smith BL, Jung JS, Agre P, Verdijk MA, et al. The human AQP4 gene: definition of the locus encoding two water channel polypeptides in brain. *Proc Natl Acad Sci U S A*. 1996 Oct 1;93(20):10908–12.
 25. de Bellis M, Cibelli A, Mola MG, Pisani F, Barile B, Mastrodonato M, et al. Orthogonal arrays of particle assembly are essential for normal aquaporin-4 expression level in the brain. *Glia*. 2021;69(2):473–88.
 26. Engel A, Fujiyoshi Y, Gonen T, Walz T. Junction-forming aquaporins. *Curr Opin Struct Biol*. 2008 Apr;18(2):229–35.
 27. Kumari SS, Varadaraj K. Intact AQP0 performs cell-to-cell adhesion. *Biochem Biophys Res Commun*. 2009 Dec 18;390(3):1034–9.
 28. Simone L, Pisani F, Mola MG, De Bellis M, Merla G, Micale L, et al. AQP4 Aggregation State Is a Determinant for Glioma Cell Fate. *Cancer Res*. 2019 May 1;79(9):2182–94.
 29. Saadoun S, Papadopoulos MC, Watanabe H, Yan D, Manley GT, Verkman AS. Involvement of aquaporin-4 in astroglial cell migration and glial scar formation. *J Cell Sci*. 2005 Dec 15;118(24):5691–8.
 30. Vasile F, Dossi E, Rouach N. Human astrocytes: structure and functions in the healthy brain. *Brain Struct Funct*. 2017;222(5):2017–29.
 31. Sofroniew MV, Vinters HV. Astrocytes: biology and pathology. *Acta Neuropathol (Berl)*. 2010;119(1):7–35.
 32. Cajal RS. *Histologie du système nerveux de l'Homme et des Vertébrés. Grand sympathique*. Paris Maloine. 1911;2:891–942.
 33. Mathiisen TM, Lehre KP, Danbolt NC, Ottersen OP. The perivascular astroglial sheath provides a complete covering of the brain microvessels: an electron microscopic 3D reconstruction. *Glia*. 2010 Jul;58(9):1094–103.
 34. Blutstein T, Haydon PG. Chapter Five - The Tripartite Synapse: A Role for Glial Cells in Modulating Synaptic Transmission. In: Pickel V, Segal M, editors. *The Synapse* [Internet]. Boston: Academic Press; 2014 [cited 2022 Aug 9]. p. 155–72. Available from:
<https://www.sciencedirect.com/science/article/pii/B9780124186750000055>
 35. Nagelhus EA, Mathiisen TM, Ottersen OP. Aquaporin-4 in the central nervous system: cellular and subcellular distribution and coexpression with KIR4.1. *Neuroscience*. 2004;129(4):905–13.

36. Mader S, Brimberg L. Aquaporin-4 Water Channel in the Brain and Its Implication for Health and Disease. *Cells*. 2019 Feb;8(2):90.
37. Waite A, Tinsley CL, Locke M, Blake DJ. The neurobiology of the dystrophin-associated glycoprotein complex. *Ann Med*. 2009 Jan 1;41(5):344–59.
38. Amiry-Moghaddam M, Frydenlund DS, Ottersen OP. Anchoring of aquaporin-4 in brain: Molecular mechanisms and implications for the physiology and pathophysiology of water transport. *Neuroscience*. 2004 Jan 1;129(4):997–1008.
39. An α -syntrophin-dependent pool of AQP4 in astroglial end-feet confers bidirectional water flow between blood and brain | PNAS [Internet]. [cited 2022 Aug 2]. Available from: <https://www.pnas.org/doi/abs/10.1073/pnas.0437946100>
40. De Bellis M, Pisani F, Mola MG, Rosito S, Simone L, Buccoliero C, et al. Translational readthrough generates new astrocyte AQP4 isoforms that modulate supramolecular clustering, glial endfeet localization, and water transport. *Glia*. 2017 May;65(5):790–803.
41. Palazzo C, Abbrescia P, Valente O, Nicchia GP, Banitalebi S, Amiry-Moghaddam M, et al. Tissue Distribution of the Readthrough Isoform of AQP4 Reveals a Dual Role of AQP4ex Limited to CNS. *Int J Mol Sci*. 2020 Feb 24;21(4):E1531.
42. Camassa LMA, Lunde LK, Hoddevik EH, Stensland M, Boldt HB, De Souza GA, et al. Mechanisms underlying AQP4 accumulation in astrocyte endfeet. *Glia*. 2015 Nov;63(11):2073–91.
43. Hoddevik EH, Rao SB, Zahl S, Boldt HB, Ottersen OP, Amiry-Moghaddam M. Organisation of extracellular matrix proteins laminin and agrin in pericapillary basal laminae in mouse brain. *Brain Struct Funct*. 2020 Mar;225(2):805–16.
44. Yamada K, Watanabe M. Cytodifferentiation of Bergmann glia and its relationship with Purkinje cells. *Anat Sci Int*. 2002 Jun;77(2):94–108.
45. Devoldere J, Peynshaert K, De Smedt SC, Remaut K. Müller cells as a target for retinal therapy. *Drug Discov Today*. 2019 Aug;24(8):1483–98.
46. Khakh BS, Deneen B. The Emerging Nature of Astrocyte Diversity. *Annu Rev Neurosci*. 2019 Jul 8;42:187–207.
47. Giaume C, Liu X. From a glial syncytium to a more restricted and specific glial networking. *J Physiol-Paris*. 2012 Jan 1;106(1):34–9.
48. Nualart-Marti A, Solsona C, Fields RD. Gap junction communication in myelinating glia. *Biochim Biophys Acta*. 2013 Jan;1828(1):69–78.
49. Papadopoulos MC, Verkman AS. Aquaporin-4 and brain edema. *Pediatr Nephrol Berl Ger*. 2007 Jun;22(6):778–84.

50. Dai W, Yan J, Chen G, Hu G, Zhou X, Zeng X. AQP4-knockout alleviates the lipopolysaccharide-induced inflammatory response in astrocytes via SPHK1/MAPK/AKT signaling. *Int J Mol Med*. 2018 Sep;42(3):1716–22.
51. Ikeshima-Kataoka H. Neuroimmunological Implications of AQP4 in Astrocytes. *Int J Mol Sci*. 2016 Aug 10;17(8):E1306.
52. Kitchen P, Salman MM, Halsey AM, Clarke-Bland C, MacDonald JA, Ishida H, et al. Targeting Aquaporin-4 Subcellular Localization to Treat Central Nervous System Edema. *Cell*. 2020 May 14;181(4):784-799.e19.
53. Prydz A, Stahl K, Zahl S, Skauli N, Skare Ø, Ottersen OP, et al. Pro-Inflammatory Role of AQP4 in Mice Subjected to Intrastratial Injections of the Parkinsonogenic Toxin MPP. *Cells*. 2020 Nov 5;9(11):E2418.
54. Sun C, Lin L, Yin L, Hao X, Tian J, Zhang X, et al. Acutely Inhibiting AQP4 With TGN-020 Improves Functional Outcome by Attenuating Edema and Peri-Infarct Astroglia After Cerebral Ischemia. *Front Immunol [Internet]*. 2022 [cited 2022 Jul 31];13. Available from: <https://www.frontiersin.org/articles/10.3389/fimmu.2022.870029>
55. Yool AJ, Brown EA, Flynn GA. Roles for novel pharmacological blockers of aquaporins in the treatment of brain oedema and cancer. *Clin Exp Pharmacol Physiol*. 2010;37(4):403–9.
56. Lourdopoulos A, Mourouzis I, Xinaris C, Zerva N, Filippakis K, Pavlopoulos A, et al. Translational Block in Stroke: A Constructive and “Out-of-the-Box” Reappraisal. *Front Neurosci [Internet]*. 2021 [cited 2022 Aug 15];15. Available from: <https://www.frontiersin.org/articles/10.3389/fnins.2021.652403>
57. Stokum JA, Kurland DB, Gerzanich V, Simard JM. Mechanisms of Astrocyte-Mediated Cerebral Edema. *Neurochem Res*. 2015 Feb;40(2):317–28.
58. Stokum JA, Gerzanich V, Simard JM. Molecular pathophysiology of cerebral edema. *J Cereb Blood Flow Metab*. 2016 Mar 1;36(3):513–38.
59. Jessen NA, Munk ASF, Lundgaard I, Nedergaard M. The Glymphatic System – A Beginner’s Guide. *Neurochem Res*. 2015 Dec;40(12):2583–99.
60. Quast MJ, Huang NC, Hillman GR, Kent TA. The evolution of acute stroke recorded by multimodal magnetic resonance imaging. *Magn Reson Imaging*. 1993 Jan 1;11(4):465–71.
61. Tait MJ, Saadoun S, Bell BA, Papadopoulos MC. Water movements in the brain: role of aquaporins. *Trends Neurosci*. 2008 Jan 1;31(1):37–43.
62. Papadopoulos MC, Manley GT, Krishna S, Verkman AS. Aquaporin-4 facilitates reabsorption of excess fluid in vasogenic brain edema. *FASEB J Off Publ Fed Am Soc Exp Biol*. 2004 Aug;18(11):1291–3.

63. Hsu Y, Tran M, Linninger AA. Dynamic regulation of aquaporin-4 water channels in neurological disorders. *Croat Med J.* 2015 Oct;56(5):401–21.
64. Spronk E, Sykes G, Falcione S, Munsterman D, Joy T, Kamtchum-Tatuene J, et al. Hemorrhagic Transformation in Ischemic Stroke and the Role of Inflammation. *Front Neurol.* 2021 May 14;12:661955.
65. Hacke W, Schwab S, Horn M, Spranger M, De Georgia M, von Kummer R. 'Malignant' Middle Cerebral Artery Territory Infarction: Clinical Course and Prognostic Signs. *Arch Neurol.* 1996 Apr 1;53(4):309–15.
66. Galea I, Bechmann I, Perry VH. What is immune privilege (not)? *Trends Immunol.* 2007 Jan 1;28(1):12–8.
67. Iadecola C, Anrather J. The immunology of stroke: from mechanisms to translation. *Nat Med.* 2011 Jul 7;17(7):796–808.
68. Jayaraj RL, Azimullah S, Beiram R, Jalal FY, Rosenberg GA. Neuroinflammation: friend and foe for ischemic stroke. *J Neuroinflammation.* 2019 Jul 10;16(1):142.
69. Bush TG, Puvanachandra N, Horner CH, Polito A, Ostefeld T, Svendsen CN, et al. Leukocyte Infiltration, Neuronal Degeneration, and Neurite Outgrowth after Ablation of Scar-Forming, Reactive Astrocytes in Adult Transgenic Mice. *Neuron.* 1999 Jun 1;23(2):297–308.
70. Yang Q qiao, Zhou J wei. Neuroinflammation in the central nervous system: Symphony of glial cells. *Glia.* 2019;67(6):1017–35.
71. Choudhury GR, Ding S. Reactive astrocytes and therapeutic potential in focal ischemic stroke. *Neurobiol Dis.* 2016 Jan;85:234–44.
72. Ikeshima-Kataoka H, Abe Y, Yasui M. Aquaporin 4-Dependent expression of glial fibrillary acidic protein and tenascin-C in activated astrocytes in stab wound mouse brain and in primary culture. *J Neurosci Res.* 2015;93(1):121–9.
73. Raznahan A, Distechi CM. X-Chromosome Regulation and Sex Differences in Brain Anatomy. *Neurosci Biobehav Rev.* 2021 Jan;120:28–47.
74. Ruigrok ANV, Salimi-Khorshidi G, Lai MC, Baron-Cohen S, Lombardo MV, Tait RJ, et al. A meta-analysis of sex differences in human brain structure. *Neurosci Biobehav Rev.* 2014 Feb;39(100):34–50.
75. Morrison HW, Filosa JA. Sex differences in astrocyte and microglia responses immediately following middle cerebral artery occlusion in adult mice. *Neuroscience.* 2016 Dec 17;339:85–99.
76. Ng YS, Stein J, Ning M, Black-Schaffer RM. Comparison of clinical characteristics and functional outcomes of ischemic stroke in different vascular territories. *Stroke.* 2007 Aug;38(8):2309–14.

77. Howells DW, Porritt MJ, Rewell SS, O'Collins V, Sena ES, van der Worp HB, et al. Different Strokes for Different Folks: The Rich Diversity of Animal Models of Focal Cerebral Ischemia. *J Cereb Blood Flow Metab.* 2010 Aug 1;30(8):1412–31.
78. Llovera G, Roth S, Plesnila N, Veltkamp R, Liesz A. Modeling Stroke in Mice: Permanent Coagulation of the Distal Middle Cerebral Artery. *J Vis Exp JoVE.* 2014 Jul 31;(89):51729.
79. Richard Green A, Odergren T, Ashwood T. Animal models of stroke: do they have value for discovering neuroprotective agents? *Trends Pharmacol Sci.* 2003 Aug 1;24(8):402–8.
80. Ribeiro M de C, Hirt L, Bogousslavsky J, Regli L, Badaut J. Time course of aquaporin expression after transient focal cerebral ischemia in mice. *J Neurosci Res.* 2006 May 15;83(7):1231–40.
81. Shin JA, Choi JH, Choi YH, Park EM. Conserved aquaporin 4 levels associated with reduction of brain edema are mediated by estrogen in the ischemic brain after experimental stroke. *Biochim Biophys Acta.* 2011 Sep;1812(9):1154–63.
82. Steiner E, Enzmann GU, Lin S, Ghavampour S, Hannocks MJ, Zuber B, et al. Loss of astrocyte polarization upon transient focal brain ischemia as a possible mechanism to counteract early edema formation. *Glia.* 2012 Nov;60(11):1646–59.
83. Filchenko I, Blochet C, Buscemi L, Price M, Badaut J, Hirt L. Caveolin-1 Regulates Perivascular Aquaporin-4 Expression After Cerebral Ischemia. *Front Cell Dev Biol.* 2020;8:371.
84. Zeng XN, Xie LL, Liang R, Sun XL, Fan Y, Hu G. AQP4 knockout aggravates ischemia/reperfusion injury in mice. *CNS Neurosci Ther.* 2012 May;18(5):388–94.
85. Coomber B, Gibson CL. Sustained levels of progesterone prior to the onset of cerebral ischemia are not beneficial to female mice. *Brain Res.* 2010 Nov 18;1361:124–32.
86. Xiong XX, Gu LJ, Shen J, Kang XH, Zheng YY, Yue SB, et al. Probenecid protects against transient focal cerebral ischemic injury by inhibiting HMGB1 release and attenuating AQP4 expression in mice. *Neurochem Res.* 2014 Jan;39(1):216–24.
87. Wang H, Chen H, Jin J, Liu Q, Zhong D, Li G. Inhibition of the NLRP3 inflammasome reduces brain edema and regulates the distribution of aquaporin-4 after cerebral ischaemia-reperfusion. *Life Sci.* 2020 Jun 15;251:117638.
88. Guo H, Yin A, Ma Y, Fan Z, Tao L, Tang W, et al. Astroglial N-myc downstream-regulated gene 2 protects the brain from cerebral edema induced by stroke. *Glia.* 2021 Feb;69(2):281–95.
89. Frydenlund DS, Bhardwaj A, Otsuka T, Mylonakou MN, Yasumura T, Davidson KGV, et al. Temporary loss of perivascular aquaporin-4 in neocortex after transient middle cerebral artery occlusion in mice. *Proc Natl Acad Sci U S A.* 2006 Sep 5;103(36):13532–6.

90. Liu X, Zhang W, Alkayed NJ, Froehner SC, Adams ME, Amiry-Moghaddam M, et al. Lack of sex-linked differences in cerebral edema and aquaporin-4 expression after experimental stroke. *J Cereb Blood Flow Metab Off J Int Soc Cereb Blood Flow Metab*. 2008 Dec;28(12):1898–906.
91. Migliati ER, Amiry-Moghaddam M, Froehner SC, Adams ME, Ottersen OP, Bhardwaj A. Na(+)-K (+)-2Cl (-) cotransport inhibitor attenuates cerebral edema following experimental stroke via the perivascular pool of aquaporin-4. *Neurocrit Care*. 2010 Aug;13(1):123–31.
92. Liu N, Shang J, Tian F, Nishi H, Abe K. In vivo optical imaging for evaluating the efficacy of edaravone after transient cerebral ischemia in mice. *Brain Res*. 2011 Jun 23;1397:66–75.
93. Chu H, Yang X, Huang C, Gao Z, Tang Y, Dong Q. Apelin-13 Protects against Ischemic Blood-Brain Barrier Damage through the Effects of Aquaporin-4. *Cerebrovasc Dis Basel Switz*. 2017;44(1–2):10–25.
94. Tang G, Liu Y, Zhang Z, Lu Y, Wang Y, Huang J, et al. Mesenchymal stem cells maintain blood-brain barrier integrity by inhibiting aquaporin-4 upregulation after cerebral ischemia. *Stem Cells Dayt Ohio*. 2014 Dec;32(12):3150–62.
95. Lo ACY, Chen AYS, Hung VKL, Yaw LP, Fung MKL, Ho MCY, et al. Endothelin-1 overexpression leads to further water accumulation and brain edema after middle cerebral artery occlusion via aquaporin 4 expression in astrocytic end-feet. *J Cereb Blood Flow Metab Off J Int Soc Cereb Blood Flow Metab*. 2005 Aug;25(8):998–1011.
96. Wang Y, Huang J, Ma Y, Tang G, Liu Y, Chen X, et al. MicroRNA-29b is a therapeutic target in cerebral ischemia associated with aquaporin 4. *J Cereb Blood Flow Metab Off J Int Soc Cereb Blood Flow Metab*. 2015 Dec;35(12):1977–84.
97. Nakano T, Nishigami C, Irie K, Shigemori Y, Sano K, Yamashita Y, et al. Goreisan Prevents Brain Edema after Cerebral Ischemic Stroke by Inhibiting Aquaporin 4 Upregulation in Mice. *J Stroke Cerebrovasc Dis Off J Natl Stroke Assoc*. 2018 Mar;27(3):758–63.
98. Hawkes CA, Michalski D, Anders R, Nissel S, Grosche J, Bechmann I, et al. Stroke-induced opposite and age-dependent changes of vessel-associated markers in co-morbid transgenic mice with Alzheimer-like alterations. *Exp Neurol*. 2013 Dec;250:270–81.
99. Yan W, Zhao X, Chen H, Zhong D, Jin J, Qin Q, et al. β -Dystroglycan cleavage by matrix metalloproteinase-2/-9 disturbs aquaporin-4 polarization and influences brain edema in acute cerebral ischemia. *Neuroscience*. 2016 Jun 21;326:141–57.
100. Mages B, Aleithe S, Blietz A, Krueger M, Härtig W, Michalski D. Simultaneous alterations of oligodendrocyte-specific CNP, astrocyte-specific AQP4 and neuronal NF-L demarcate ischemic tissue after experimental stroke in mice. *Neurosci Lett*. 2019 Oct 15;711:134405.

101. Liu L, Vollmer MK, Kelly MG, Fernandez VM, Fernandez TG, Kim H, et al. Reactive Gliosis Contributes to Nrf2-Dependent Neuroprotection by Pretreatment with Dimethyl Fumarate or Korean Red Ginseng Against Hypoxic-Ischemia: Focus on Hippocampal Injury. *Mol Neurobiol.* 2020 Jan;57(1):105–17.
102. Cui X, Chopp M, Zacharek A, Karasinska JM, Cui Y, Ning R, et al. Deficiency of brain ATP-binding cassette transporter A-1 exacerbates blood-brain barrier and white matter damage after stroke. *Stroke.* 2015 Mar;46(3):827–34.
103. Monai H, Wang X, Yahagi K, Lou N, Mestre H, Xu Q, et al. Adrenergic receptor antagonism induces neuroprotection and facilitates recovery from acute ischemic stroke. *Proc Natl Acad Sci U S A.* 2019 May 28;116(22):11010–9.
104. Sanchez-Bezanilla S, TeBay C, Nilsson M, Walker FR, Ong LK. Visual discrimination impairment after experimental stroke is associated with disturbances in the polarization of the astrocytic aquaporin-4 and increased accumulation of neurotoxic proteins. *Exp Neurol.* 2019 Aug;318:232–43.
105. Zhang J, Zhao H, Xue Y, Liu Y, Fan G, Wang H, et al. Impaired Glymphatic Transport Kinetics Following Induced Acute Ischemic Brain Edema in a Mouse pMCAO Model. *Front Neurol.* 2022;13:860255.
106. Banitalebi S, Skauli N, Geiseler S, Ottersen OP, Amiry-Moghaddam M. Disassembly and Mislocalization of AQP4 in Incipient Scar Formation after Experimental Stroke. *Int J Mol Sci.* 2022 Jan 20;23(3).
107. Li SY, Yang D, Yeung CM, Yu WY, Chang RCC, So KF, et al. Lycium barbarum polysaccharides reduce neuronal damage, blood-retinal barrier disruption and oxidative stress in retinal ischemia/reperfusion injury. *PloS One.* 2011 Jan 26;6(1):e16380.
108. Dutta S, Sengupta P. Men and mice: Relating their ages. *Life Sci.* 2016 May 1;152:244–8.
109. Aoki K, Uchihara T, Tsuchiya K, Nakamura A, Ikeda K, Wakayama Y. Enhanced expression of aquaporin 4 in human brain with infarction. *Acta Neuropathol (Berl).* 2003 Aug 1;106(2):121–4.
110. Satoh J ichi, Tabunoki H, Yamamura T, Arima K, Konno H. Human astrocytes express aquaporin-1 and aquaporin-4 in vitro and in vivo. *Neuropathol Off J Jpn Soc Neuropathol.* 2007 Jun;27(3):245–56.
111. Mogoanta L, Ciurea M, Pirici I, Margaritescu C, Simionescu C, Ion DA, et al. Different dynamics of aquaporin 4 and glutamate transporter-1 distribution in the perineuronal and perivascular compartments during ischemic stroke. *Brain Pathol Zurich Switz.* 2014 Sep;24(5):475–93.
112. Stokum JA, Mehta RI, Ivanova S, Yu E, Gerzanich V, Simard JM. Heterogeneity of aquaporin-4 localization and expression after focal cerebral ischemia underlies differences in white versus grey matter swelling. *Acta Neuropathol Commun.* 2015 Sep 30;3:61.

113. Roșu GC, Pirici I, Istrate-Ofițeru AM, Iovan L, Tudorică V, Mogoantă L, et al. Expression patterns of aquaporins 1 and 4 in stroke. *Romanian J Morphol Embryol Rev Roum Morphol Embryol*. 2019;60(3):823–30.
114. Kleffner I, Bungeroth M, Schiffbauer H, Schäbitz WR, Ringelstein EB, Kuhlenbäumer G. The role of aquaporin-4 polymorphisms in the development of brain edema after middle cerebral artery occlusion. *Stroke*. 2008 Apr;39(4):1333–5.
115. Marazuela P, Bonaterra-Pastra A, Faura J, Penalba A, Pizarro J, Pancorbo O, et al. Circulating AQP4 Levels in Patients with Cerebral Amyloid Angiopathy-Associated Intracerebral Hemorrhage. *J Clin Med*. 2021 Mar 2;10(5).
116. Rosu GC, Pirici I, Grigorie AA, Istrate-Ofițeru AM, Iovan L, Tudorica V, et al. Distribution of Aquaporins 1 and 4 in the Central Nervous System. *Curr Health Sci J*. 2019 Jun;45(2):218–26.
117. Jung JS, Bhat RV, Preston GM, Guggino WB, Baraban JM, Agre P. Molecular characterization of an aquaporin cDNA from brain: candidate osmoreceptor and regulator of water balance. *Proc Natl Acad Sci*. 1994 Dec 20;91(26):13052–6.
118. Hasegawa H, Ma T, Skach W, Matthay MA, Verkman AS. Molecular cloning of a mercurial-insensitive water channel expressed in selected water-transporting tissues. *J Biol Chem*. 1994 Feb 25;269(8):5497–500.
119. Solenov E, Watanabe H, Manley GT, Verkman AS. Sevenfold-reduced osmotic water permeability in primary astrocyte cultures from AQP-4-deficient mice, measured by a fluorescence quenching method. *Am J Physiol Cell Physiol*. 2004 Feb;286(2):C426-432.
120. Manley GT, Fujimura M, Ma T, Noshita N, Filiz F, Bollen AW, et al. Aquaporin-4 deletion in mice reduces brain edema after acute water intoxication and ischemic stroke. *Nat Med*. 2000 Feb;6(2):159–63.
121. Amiry-Moghaddam M, Otsuka T, Hurn PD, Traystman RJ, Haug FM, Froehner SC, et al. An alpha-syntrophin-dependent pool of AQP4 in astroglial end-feet confers bidirectional water flow between blood and brain. *Proc Natl Acad Sci U S A*. 2003 Feb 18;100(4):2106–11.
122. Pati R, Palazzo C, Valente O, Abbrescia P, Messina R, Surdo NC, et al. The Readthrough Isoform AQP4ex Is Constitutively Phosphorylated in the Perivascular Astrocyte Endfeet of Human Brain. *Biomolecules*. 2022 Apr 25;12(5):633.
123. Rustenhoven J, Aalderink M, Scotter EL, Oldfield RL, Bergin PS, Mee EW, et al. TGF-beta1 regulates human brain pericyte inflammatory processes involved in neurovasculature function. *J Neuroinflammation*. 2016 Feb 11;13:37.
124. Vafadari B, Salamian A, Kaczmarek L. MMP-9 in translation: from molecule to brain physiology, pathology, and therapy. *J Neurochem*. 2016;139(S2):91–114.